Available online at www.sciencedirect.com

ScienceDirect

IFAC PapersOnline CONFERENCE PAPER ARCHIVE

IFAC PapersOnLine 52-21 (2019) 242–247

Trajectory generation and tracking on $SE(3)$ for an underactuated AUV with disturbances

Helen C. Henninger[1] * **Karl D. von Ellenrieder** ** **and James D. Biggs** ***

* *Free University of Bozen-Bolzano, Bolzano, Italy, 39100 (e-mail: HelenClare.Henninger@unibz.it)*
** *Free University of Bozen-Bolzano, Bolzano, Italy, 39100*
*** *Politecnico di Milano, Milan, Italy, 20133*

Abstract: This paper describes the trajectory tracking of an underactuated autonomous underwater vehicle (AUV) with three control inputs (surge, yaw and pitch moment) that operates in the presence of time-varying disturbances. The AUV kinematics are described in global coordinates as a Hamiltonian system on the Lie group $SE(3)$ and the boundary-value problem arising from the geometric framing of Pontryagin's Maximum Principle is applied to the vehicle kinematics. This 6-dimensional boundary value problem is solved using a numerical shooting method and a novel semi-analytical Lie group integrator. The integrator uses Rodrigue's formula to express the exact solution of the solution curves, is symplectic and preserves energy and momentum. Inverse dynamics is applied to construct an inner-loop controller, which accounts for constraints on maximum torque and force via time reparametrization. This inner-loop control, which would drive the AUV along the reference trajectory in perfect conditions, is combined with a disturbance observer to construct an outer-loop controller, which ensures stability in the presence of bounded disturbances. Simulation results complete the work.

Keywords: Marine systems, geometric control, disturbances, integral windup, stability

1. INTRODUCTION

The control of an AUV is challenging. The dynamic equations are nonlinear and generally underactuated. In addition, uncertain dynamics introduced from the environment can cause failure of control laws that were designed under ideal circumstances. In the case of manoueverable vehicles (i.e.vehicles required to undergo large ranges of motion in 3-D space), limitations may also arise from control schemes themselves: traditional control schemes based on local motion parametrizations (like Euler angle descriptions) artificially limit the range of motion due to singularities. Thus, a global description, such as a Lie group model, is preferred. For example Nui & Geng (2016) present the stabilization of a relative equilibrium for an underactuated AUV in the context of Hamiltonian systems on the Lie group $SE(3)$ with physical damping terms. A 2-part control law is derived by reshaping the kinetic energy and reassigning damping terms via the Simultaneous Interconnection and Damping Assignment (SIDA) Method to globally stabilize an underactuated AUV that moves along its longitudinal axis where the body velocity is given in terms of an arbitrary parameter. The optimal control of an underactuated autonomous underwater vehicle is considered in Biggs & Holderbaum (2009). The kinematics are modeled on $SE(3)$ and the integral of a quadratic function of the velocity components is minimized by applying Pontryagin's Maximum Principle (PMP). A special case of the cost function for which optimal motions trace helical paths is considered. The dynamics are not taken into account and an approach for numerically computing the parameters to match the boundary conditions is not provided. Yoerger & Slotine (1985) consider a conventional sliding-mode controller on $SE(3)$, which has steady-state error when the AUV is exposed to constant disturbances, such as currents and buoyancy. In Candeloro et al. (2013), a two-dimensional curvature-continuous path planning algorithm is presented based on Voronoi diagrams and Fermat's spiral segments; it respects kinematic and dynamic constraints by setting a maximum threshold for the path curvature to construct a simple path composed of straight lines and spiral segments. However, an optimization method based on PMP may be used to produce similarly simple paths. Viswanathan et al (2015) use desired waypoints for the translational motion and a desired trajectory for the attitude, based on the desired thrust direction to generate a trajectory for an underactuated AUV with four control inputs modelled on $SE(3)$. The effects of disturbances along the uncontrolled axes are considered. A feedback control law is obtained to steer the underactuated vehicle towards the desired trajectories, taking into account known bounds on the control inputs.

The numerical integration of systems evolving on Lie groups requires symplectic integrators capable of preserv-

[1] This work was sponsored by the European Regional Development Fund (FiRST Lab Project # FESR 1084)

10.1016/j.ifacol.2019.12.314

ing Hamiltonian and group structures. Discrete-time analogues of Lagrangian and Hamiltonian mechanics derived from discrete variational principles yield a class of geometric numerical integrators, which are referred to as variational integrators. These are often used for constructing symplectic numerical integrators for discrete Lagrangians or Hamiltonians that are group-invariant. The numerical method is also momentum preserving. Such an approach is developed in Lee et al (2007). The discretization scheme of Lee et al (2007) based on the discrete Lagrange-d'Alembert principle is extended to obtain the Lie group variational integrator which is applied to a conservative underwater system. This method is applied in Nordkvist & Sanyal (2010), which creates a Lie group variational integrator for the full (translation and orientation) motion of a rigid body under the possible influence of nonconservative forces and torques. This integrator is also applied in the paper Sanyal et al (2011) for tracking a desired continuous trajectory for a maneuverable autonomous vehicle in the presence of gravity, buoyancy and fluid dynamic forces and moments. The paper Henninger & Biggs (2018) gives a theoretical and very general method of designing an optimal trajectory using a global semi-analytical Lie group integrator, but does not consider tracking of this trajectory and does not include any dynamics, both of which are required for applications in the control of marine systems. However, unlike variational methods, this can be adapted using Rodrigue's formula to achieve conservation of energy, momentum and symplectic structure using the exact solutions. The iterative integration method preserves the first integral and group structure and so makes the method viable for trajectories with a long time duration, where other integrators fail to preserve the group structure over long time intervals and so lose accuracy (Bloch et al., 2009).

Highly maneuverable AUVs are being developed, including miniature aerial and underwater vehicles that can be operated in large ranges of motion. For example, the performance of miniature autonomous underwater vehicles (Pan & Zhu (2003)) and the REMUS AUV have been improved for more manoueverable operation. However, inherently agile AUVs that undergo complex multiaxis motions that accentuate nonlinearities- including disturbance terms - (Yoerger & Slotine, 1985) would operate better under ideal conditions. Controls which are adapted to handle unknown exogenous disturbances would be especially practical for these kinds of vehicles. In many problems of practical importance, unknown exogenous disturbances, as well as model uncertainty of the plant and actuators canbe significant. When disturbance observer based control (DOBC) design methods Chen & Guo (2014), Chen et al (2016) are used, the exogenous disturbances and uncertainty can be combined and treated as an overall disturbance term.

Our aim in this paper is to produce an optimal trajectory between two points for the AUV and to construct a controller that is stable under disturbances. We will follow many of the references cited above in describing the system kinematics on $SE(3)$, and then formulate the problem as an optimal kinematic control problem on a matrix Lie group. An application of PMP gives the necessary conditions for optimality in the form of extremal equations. This has the advantage that simple paths can be derived. In fact, for maneuvers in 2 dimensions these are Dubins curves (Jurdjevic, 1997). The extremal equations and the trajectories are expressed in global coordinates by adapting the iterative Lie group method developed in Henninger & Biggs (2018) using Rodrigue's formula for the case of $SE(3)$. The method of inverse dynamics is then applied to the resulting velocities to ensure that the constraints on the maximum forces and torques are satisfied in the inner-loop control. Finally, using inverse dynamics, no anti-windup is needed in the inner-loop control because this approach keeps the control force magnitude within the bounds of the controllers. However, inner-loop controls have generally been found to be highly sensitive to uncertainties and disturbances. To reduce these errors, we construct an outer-loop control, which has as an inner loop the control constructed using the PMP where the disturbances are estimated using a disturbance observer (Do, 2010; Du et al, 2016; Wu et al, 2014). This control is shown to be Lyapunov-stable. The use of a Lie group symplectic integrator to generate optimal trajectories and combine this with a stabilizing tracking controller for an AUV in the presence of disturbances is novel.

This paper is organized as follows. In Section 2 we describe the model on $SE(3)$ and the methods used to determine the inner-loop (Section 2.1) and outer-loop (Section 2.2) controller; the parameters used for the simulations are listed in Section 3 where the simulation results are presented and discussed. Section 4 is the conclusion.

2. METHOD

In this section we describe the system kinematics and dynamics and then formulate the trajectory generation problem as an optimal kinematic control problem on a matrix Lie group. An application of PMP gives the necessary conditions for optimality in the form of extremal equations. We describe the Lie group integration method for finding the trajectory in $SE(3)$ and explain how inverse dynamics are applied to meet the the force and torque constraints in the inner-loop control. Lastly, the disturbance observer for outer- loop control is described.

2.1 Kinematics and dynamics

The maneuverable autonomous underwater vehicle is kinematically modelled as a submerged rigid body. We assume three planes of symmetry and that the geometric center and the center of gravity G are coincident, so that we can neglect moments generated by the drag force and so that the propeller line of action lies along G . Following Nui & Geng (2016), Sanyal et al (2011) and Fossen & Berge (2011), the configuration of the rigid body is modelled on $SE(3)$, which is the semi-direct product $(\mathbf{r}, R)$ by $g \in SE(3)$, where $\mathbf{r}$ denotes the inertial position vector and R denotes the body orientation (attitude) in the body frame. The pair $(\mathbf{r}, R)$ can be written in the more familar form

$$\boldsymbol{\eta} = [x \ y \ z \ \phi \ \theta \ \psi], \tag{1}$$

where we extract the Euler angles ϕ, θ, ψ from the rotation matrix $R(t)$ in the usual way. Since we wish to avoid the Euler angle parametrization in favor of a global representation, this expression will not be used in our computations. The kinematic equations for a rigid body are given by

$$\dot{\mathbf{r}} = R\boldsymbol{\nu} \quad \text{and} \quad \dot{R} = R\Omega, \tag{2}$$

where the translation and angular velocities in the body-fixed frame are denoted by $\boldsymbol{\nu} = [\nu_1, \nu_2, \nu_3]$ and $\Omega = [\omega_1, \omega_2, \omega_3]^T$, respectively. We write these as $\widetilde{\Omega} = (\boldsymbol{\nu}, \Omega)$ where $\widetilde{\Omega}$ is an element of the vector space $\mathfrak{se}(3)$. The Lie algebra of $SE(3)$, is given by

$$\mathfrak{se}(3) = \left\{ \begin{bmatrix} 0 & -x_6 & x_4 & x_1 \\ x_6 & 0 & -x_5 & x_2 \\ -x_4 & x_5 & 0 & x_3 \\ 0 & 0 & 0 & 0 \end{bmatrix} \mid x_1, x_2, x_3, x_4, x_5, x_6 \right\}, \quad (3)$$

which is spanned by the basis

$$B_1 = \begin{bmatrix} 0&0&0&1 \\ 0&0&0&0 \\ 0&0&0&0 \\ 0&0&0&0 \end{bmatrix}, B_2 = \begin{bmatrix} 0&0&0&0 \\ 0&0&0&1 \\ 0&0&0&0 \\ 0&0&0&0 \end{bmatrix}, B_3 = \begin{bmatrix} 0&0&0&0 \\ 0&0&0&0 \\ 0&0&0&1 \\ 0&0&0&0 \end{bmatrix},$$

$$B_4 = \begin{bmatrix} 0&0&1&0 \\ 0&0&0&0 \\ -1&0&0&0 \\ 0&0&0&0 \end{bmatrix}, B_5 = \begin{bmatrix} 0&0&0&0 \\ 0&0&-1&0 \\ 0&1&0&0 \\ 0&0&0&0 \end{bmatrix}, B_6 = \begin{bmatrix} 0&-1&0&0 \\ 1&0&0&0 \\ 0&0&0&0 \\ 0&0&0&0 \end{bmatrix}. \quad (4)$$

We assume that the origin of the body fixed frame is at the center of gravity. The equation of motion representing the dynamics is

$$\mathbf{M}\dot{\boldsymbol{V}} = -C(\boldsymbol{V})\boldsymbol{V} - D(\boldsymbol{V})\boldsymbol{V} - \mathbf{g}(g) + \boldsymbol{\tau} + \boldsymbol{d}, \quad (5)$$

where

$$\mathbf{M} = \begin{bmatrix} m\mathbf{1} + M_f & 0 \\ 0 & I_b + I_f \end{bmatrix}$$

for m is the mass of the rigid body, $\mathbf{1}$ is the 3×3 identity matrix, I_b the body inertia matrix, and M_f,I_f are respectively referred to as the added mass and the added moment of inertia. We can denote the inertia tensor related to this quadratic form as M, $\boldsymbol{V} = [\boldsymbol{\omega}(t), \boldsymbol{v}(t)]^\top$, $C(\boldsymbol{V})$ is the Coriolis and centripetal matrix, $D(\boldsymbol{V})$ is the damping matrix, $\mathbf{g}(g)$ is the gravity-induced forces and moments, $\boldsymbol{\tau}$ are the actuator forces/moments and $\boldsymbol{d}$ is the vector representing the disturbance forces and torques acting on the vehicle. We can simplify (5) as

$$M\dot{\boldsymbol{V}} = \boldsymbol{\tau} + \boldsymbol{N}(\boldsymbol{V}, g) + \boldsymbol{d}, \quad (6)$$

where $\boldsymbol{N}(\boldsymbol{V}, g)$ contains the Coriolis and centripetal, damping and gravity-induced terms. In the absence of disturbances, this simplifies to

$$M\dot{\boldsymbol{\nu}} = \boldsymbol{\tau} + \boldsymbol{N}(\boldsymbol{V}, g). \quad (7)$$

2.2 Trajectory generation

The problem of moving the AUV from a given initial position to a given final position is described by the optimal control problem

$$\begin{cases} \dot{g}(t) & = g(t)\widetilde{\Omega}(t), \\ g(0) & = g_0, \quad g(t_f) = g_d \end{cases} \quad (8)$$

where $g = (\mathbf{r}, R) \in SE(3)$. In this section, we derive an analytic form of the optimal motion and the required (inner-loop) control forces. To derive this inner-loop control, we will solve (8) as an optimal control problem, where in addition to the boundary conditions, the velocities $\boldsymbol{V}(t)$ must satisfy the quadratic cost

$$\mathcal{J} = \int_0^{t_f} \boldsymbol{V} C(c_i) \boldsymbol{V}^T dt. \quad (9)$$

where $C(c_i) = \mathrm{diag}(c_1, c_2, ..., c_6)$. While this cost is primarily chosen because it gives rise to a smooth Hamiltonian and so to smooth expressions of the velocities, forces and torques, it is also practical in the following sense. Writing the cost (9) as a metric $\mathcal{J}(\boldsymbol{V}) = \|\boldsymbol{V}\|_C$ and the kinetic energy metric as $\|\boldsymbol{V}\|_T = \boldsymbol{V}^T M \boldsymbol{V}$, we note that we may always find some c_i such that

$$\|\boldsymbol{V}\|_{C(c_i)} \leq \|\boldsymbol{V}\|_T \quad (10)$$

In fact, to ensure that the choice of c_i is not trivial (for example machine epsilon), we may choose c_i such that

$$C_i(\boldsymbol{V}) = \max_{c_i \in \mathbb{R}} (\|\boldsymbol{V}\|_{C(c_i)} \leq \|\boldsymbol{V}\|_T) \quad (11)$$

for a given curve $\boldsymbol{V}$. Thus, for these C_i we note that any curve minimizing $\mathcal{J}$ will also result in a minimum-energy curve for the AUV as measured by the metric $\|\cdot\|_T$.To this optimal control problem (8) , (9) we will then apply Pontryagin's Maximum Principle. The Pontryagin Maximum Principle is a necessary condition for optimality which associates to (8) with the cost (9) an optimal Hamiltonian function H on the Lie algebra $\mathfrak{se}(3)$, and the extremal equations in terms of $P_1, P_2, ..., P_6 \in \mathfrak{se}(3)$ where $P_i = p(B_i)$ for $p(\cdot)$ a scalar function mapping the Lie algebra to its dual defined through a non-degenerate trace form.

In Henninger & Biggs (2018), a generalized case of (8)-(9) is considered, where instead of $g \in SE(3)$, g is in the so-called generalized ϵ group, and $\widetilde{\Omega}$ is replaced with an element $\sum_{i=1}^{6} x_i E_i$ where E_i is in the ϵ-Lie algebra $\mathfrak{g}_\epsilon$ with the basis

$$E_1 = \begin{bmatrix} 0&0&0&1 \\ 0&0&0&0 \\ 0&0&0&0 \\ -\epsilon&0&0&0 \end{bmatrix}, E_2 = \begin{bmatrix} 0&0&0&0 \\ 0&0&0&1 \\ 0&0&0&0 \\ 0&-\epsilon&0&0 \end{bmatrix}, E_3 = \begin{bmatrix} 0&0&0&0 \\ 0&0&0&0 \\ 0&0&0&1 \\ 0&0&-\epsilon&0 \end{bmatrix}$$

$$E_4 = \begin{bmatrix} 0&0&1&0 \\ 0&0&0&0 \\ -1&0&0&0 \\ 0&0&0&0 \end{bmatrix}, E_5 = \begin{bmatrix} 0&0&0&0 \\ 0&0&-1&0 \\ 0&1&0&0 \\ 0&0&0&0 \end{bmatrix}, E_6 = \begin{bmatrix} 0&-1&0&0 \\ 1&0&0&0 \\ 0&0&0&0 \\ 0&0&0&0 \end{bmatrix}.$$

Note that when $\epsilon = 0$, this Lie algera coincides with $\mathfrak{se}(3)$. For the cases $\epsilon = 1, -1$ in the optimal control problem (8), (9) , it is well-known that the extremal equations arising from PMP on $\mathfrak{g}_\epsilon$ take the Lax-pair form $\dot{P} = [p(\widetilde{\Omega}), P]$, where $[\cdot, \cdot]$ is the Lie bracket. From Henninger & Biggs (2018) we have the following description of the extremal equations of the optimal control problem (8):

Proposition For optimal control problems of the form (8), (9) , the extremal is the solution of

$$\begin{cases} \dot{g} & = g(t) dH \\ \dot{h}k & = [h^k, \widetilde{\Omega}_k] + \frac{1}{\epsilon}[\epsilon h^\epsilon, \widetilde{\Omega}_\epsilon], \\ \epsilon \dot{h}_\epsilon & = [\epsilon h^\epsilon, \widetilde{\Omega}_k] + \epsilon [h^k, \widetilde{\Omega}_\epsilon], \end{cases} \quad (12)$$

as $\lim \epsilon \to 0$ where $h \in \mathfrak{g}$, $h = h^k + h^\epsilon$, $h^k = h_{m+1}E_{m+1} + ... + h_n E_n$. □

This means that by taking a very small ϵ (for our purposes we take $\epsilon = 1 \times 10^{-10}$), we may apply this form of the extremal equations to solve (12) iteratively. We now apply Rodrigue's formula to describe the form of the solution:

Theorem 1 The solution curve $(g(t), (\boldsymbol{v}(t), \boldsymbol{\omega}(t)))$of the optimal control problem (8), (9) is given by the iterative scheme

$$
\begin{aligned}
g^{i+1} &= (I + \widetilde{\Omega}^i \sin(n) + (\widetilde{\Omega}^i)2(1-\cos(n)))g^i,\\
P^{i+1} &= (I + \widetilde{\Omega}^i \sin(n) + (\widetilde{\Omega}^i)^2(1-\cos(n)))P^i(I + \widetilde{\Omega}^i \sin(n)\\
&\qquad + (\widetilde{\Omega}^i)^2(1-\cos(n))) - 1,\\
\widetilde{\Omega}^i &= (P^i_{13}A_4 + P^i_{23}A_5 + P^i_{12}A_6)\\
&\qquad + \lim_{\epsilon\to 0}\frac{1}{\epsilon}(P^i_{14}A_1 + P^i_{24}A_2 + P^i_{34}A_3),
\end{aligned}
$$

where n is a chosen step-size, $t_i = n \cdot i$,

$$P(t) = \epsilon \sum_{j=1}^{3} \rho_j \boldsymbol{\omega}^j(t) A_{j+3} + \epsilon(\sum_{j=1}^{3} \boldsymbol{v}^i(t) A_j),$$

and the initial step values are

- $\widetilde{\Omega}(0) = \sum_{j=1}^{3} \rho_j \boldsymbol{\omega}^j(0) A_{j+3} + (\sum_{j=1}^{3} \boldsymbol{v}^i_e(0) A_j)$,
- $P^0 = \sum_{j=1}^{3} \rho_j \boldsymbol{\omega}^j(0) A_{j+3} + (\sum_{j=1}^{3} \boldsymbol{v}^i(0) A_j)$,
- $g^0 = g(0)$

for $A_i = \frac{1}{\epsilon}E_i$, $i = 1, 2, 3$ and $A_i = E_i$ for $i = 4, 5, 6$.

Proof 1. The form of the solution of (12) given in Henninger & Biggs (2018) (equation (16)) is

$$
\begin{aligned}
g^{i+1} &= g^i \exp(\widetilde{\Omega}^i n)\\
P^{i+1} &= \exp(\widetilde{\Omega}^i n)^{-1} P^i \exp(\widetilde{\Omega}^i n)\\
\widetilde{\Omega}^i &= (P^i_{13}A_4 + P^i_{23}A_5 + P^i_{12}A_6)\\
&\qquad + \lim_{\epsilon\to 0}\frac{1}{\epsilon}(P^i_{14}A_1 + P^i_{24}A_2 + P^i_{34}A_3).
\end{aligned}
$$

But, by Rodrigue's formula, we have the explicit form of the exponential for each i,

$$\exp(\widetilde{\Omega}^i) = (I + \widetilde{\Omega}^i \sin(n) + (\widetilde{\Omega}^i)2(1-\cos(n))).$$

2.3 Inner-loop control

The following steps are used to solve the constrained problem of moving the vehicle from the initial to the final configuration. These steps are applied in the absence of disturbance forces/torques to design the inner-loop control under ideal conditions, i.e. the dynamics are given by (7). The disturbance forces/torques in (6) are introduced in the next section where we design the outer-loop control.

- *Step 1*: Determine the solution $g(t, P^0), P(t, P^0)$ of (8) with the cost (9) using (13) in terms of the unknown boundary conditions $P^0 = (\boldsymbol{v}^0, \boldsymbol{\omega}^0)$ and on the virtual time domain $t \in [0, 1]$ (this scaled time is denoted t to differentiate it from real time $e \in [0, T_f]$).
- *Step 2*: Construct the "error vector" $\widetilde{\boldsymbol{\eta}}(1, P^0) = \boldsymbol{\eta}(g(1, P^0)) - \boldsymbol{\eta}_d$ and the function
$$S(P^0) = \|\widetilde{\boldsymbol{\eta}}(1, P^0)\|. \tag{13}$$
- *Step 3*: Find P^0 that minimizes $S(P^0)$using a minimizer, such as Matlab's `fminunc`.
- *Step 4*: Apply the method of inverse dynamics, making use of the "feasibility" time reparametrization
$$F(\cdot) : [0, T_f] \to [0, 1], \quad F(\widetilde{t}) = \widetilde{t}/T_f. \tag{14}$$
Here, T_f is the true final time, and a new rotation and translation is defined as $R^*(\widetilde{t}) = R(F(\widetilde{t}))$, $x^*(\widetilde{t}) = x(F(\widetilde{t}))$ and the corresponding angular and linear velocities are
$$\boldsymbol{V}^*(\widetilde{t}) = \frac{1}{T_f}\boldsymbol{V}(F(\widetilde{t})). \tag{15}$$

Equation (14) is used to numerically compute $\boldsymbol{T}(\widetilde{t})$ on the interval $[0, T_f]$ for some time guess T_f. The time T_f is then tuned to bring the magnitude $|\boldsymbol{T}(\widetilde{t})|$ within the constraints on the maximum force and torque.

2.4 Outer- loop control

In this section a tracking controller is developed to track the generated attitude motions in the presence of environmental disturbances. This is related to the Singular Stabilization Controls Method described in Horri & Palmer (2012), but extends to the tracking problem. A disturbance observer is constructed using the approach presented in (Wu et al, 2014). The disturbance estimate is computed as

$$\hat{\mathbf{d}} = \mathbf{q}(t) + K_0 M \mathbf{V}, \tag{16}$$

where

$$\dot{\mathbf{q}}(t) = -K_0\mathbf{q}(t) - K_0[N(\nu, \eta) + \tau(u) + K_0 M\nu], \tag{17}$$

and $K_0 = K_0^T > 0$. We define the disturbance estimation error as

$$\widetilde{\mathbf{d}} = \widehat{\mathbf{d}} - \mathbf{d}. \tag{18}$$

As proven in Do (2010), choosing the Lyapunov function candidate

$$V_{d0} = \frac{1}{2}\widetilde{\mathbf{d}}^T\widetilde{\mathbf{d}} = \frac{1}{2}\|\widetilde{\mathbf{d}}\|^2, \tag{19}$$

since both $V_{d0}(t)$ and $\widetilde{\mathbf{d}}s$ are globally uniformly ultimately bounded such that

$$0 \le V_{d0} \le \frac{C_d}{2\alpha} + \left[V_{d0} - \frac{C_d}{2\alpha}\right] e^{-2\alpha t} \tag{20}$$

and

$$\|\widetilde{\mathbf{d}}\| \le \sqrt{\frac{C_d}{2\alpha} + 2\left[V_{d0} - \frac{C_d}{2\alpha}\right] e^{-2\alpha t}}, \tag{21}$$

the disturbance error settles to within a compact set that can be made arbitrarily small by appropriately selecting K_0.

We develop the inner-loop for the controller, which defines $\boldsymbol{V}^*$ and g^* . The "virtual trajectory" g^* is obtained by applying the inner-loop controller τ_d to the system. We will denote the trajectory arising after the outer-loop control is applied to the perturbed system with dynamics (6) by g and the corresponding velocities by $\boldsymbol{V}$; the error function in this case is

$$\widetilde{\boldsymbol{V}} = \boldsymbol{V} - \boldsymbol{V}^*.$$

Note that from (13), if $\widetilde{\boldsymbol{V}} \to 0$, then $\widetilde{\boldsymbol{\eta}} \to 0$ by definition, and so we do not need to include the position error $\widetilde{\boldsymbol{\eta}}$ further in our computations to track position.

We now construct the outer-loop control

$$\boldsymbol{\tau} = -k_3(\boldsymbol{V} - \boldsymbol{V}^*) + K\dot{\boldsymbol{V}}^* - \boldsymbol{N}(\boldsymbol{V}, g) - \hat{\mathbf{d}}, \tag{22}$$

which provides stability in the presence of bounded disturbances. Particularly, we have the Lyapunov candidate function

$$V = \langle\widetilde{\boldsymbol{V}}, K\widetilde{\boldsymbol{V}}\rangle. \tag{23}$$

Taking the derivative gives

$$\dot{V} = \widetilde{\boldsymbol{V}}K\dot{\widetilde{\boldsymbol{V}}} = \langle\boldsymbol{V} - \boldsymbol{V}^*, K\dot{\boldsymbol{V}} - K\dot{\boldsymbol{V}}^*\rangle,$$

where from (6) we know that $K\dot{\boldsymbol{V}} = \boldsymbol{\tau} + \boldsymbol{N}(\boldsymbol{V}, g) + \mathbf{d}$. Thus

$$\dot{V} = \langle \boldsymbol{V} - \boldsymbol{V}^*, \boldsymbol{\tau} + \boldsymbol{N}(\boldsymbol{V}, g) - K\dot{\boldsymbol{V}}^* \rangle$$

But from the controller (22), we see that

$$K\dot{\boldsymbol{V}}^* = \boldsymbol{\tau} + k_3(\boldsymbol{V} - \boldsymbol{V}^*) + \boldsymbol{N}(\boldsymbol{V}, g) + \widehat{\mathbf{d}},$$

and so

$$\begin{aligned}\dot{V} &= \langle \boldsymbol{V} - \boldsymbol{V}^*, (-k_3(\boldsymbol{V} - \boldsymbol{V}^*) + (\mathbf{d} - \hat{\mathbf{d}}) \rangle \\ &\leq \langle \boldsymbol{V} - \boldsymbol{V}^*, -k_3(\boldsymbol{V} - \boldsymbol{V}^*) \rangle + \frac{1}{2}\langle \boldsymbol{V} - \boldsymbol{V}^*, (\boldsymbol{V} - \boldsymbol{V}^*) \rangle \\ &\quad + \frac{1}{2}\langle (\mathbf{d} - \hat{\mathbf{d}}), (\mathbf{d} - \hat{\mathbf{d}}) \rangle \\ &= (-k_3 + \frac{1}{2})\langle \boldsymbol{V} - \boldsymbol{V}^*, \boldsymbol{V} - \boldsymbol{V}^* \rangle - \frac{1}{2}\langle \widetilde{\boldsymbol{d}}, \widetilde{\boldsymbol{d}} \rangle\end{aligned}$$

where Young's inequality is applied. Thus, locally about the equilibrium point $g = 0$, $\boldsymbol{V} = 0$, we see that $\dot{V} < 0$ for any positive $k_3 > 1/2$. The desired state is locally asymptotically stable.

3. SIMULATIONS

The performance of the control law (22) is investigated using a simulation of a REMUS AUV tracking the constructed trajectory in the presence of disturbances. The maneuvering coefficients and physical characteristics of the AUV were obtained from Prestero (2001) and are given in table 1. The maximum thrust is taken as $7N$.

Table 1: Parameter values used in the simulation.

Param	Value	Param	Value
W	$320\ kg$	$Y_{\dot{r}}$	$-1.93\ kg \cdot m/\text{rad}$
I_x	$1.77 \times 10^{-1}\ kg \cdot m^2$	$Y_{\dot{v}}$	$-3.55 \times 10^{1}\ kg$
I_y	$3.45\ kg \cdot m^2$	$Z_{\dot{w}}$	$-3.55 \times 10^{1}\ kg$
I_z	$3.45\ kg \cdot m^2$	$Z_{\dot{q}}$	$-1.93\ kg \cdot m/\text{rad}$
$M_{\dot{q}}$	$-4.88\ kg \cdot m^2/\text{rad}$	$K_{\dot{p}}$	$-7.04 \times 10^{-2} kg \cdot m^2/\text{rad}$
$M_{\dot{w}}$	$-1.93\ kg \cdot m$	$N_{\dot{r}}$	$-4.88\ kg \cdot m/\text{rad}$
$X_{\dot{u}}$	$-9.30 \times 10^{-1}\ kg$	$N_{\dot{v}}$	$-1.93\ kg \cdot m$

We apply the steps described n to create a path for the AUV starting from initial configuration g_0 to final configuration g_d, where

$$g_0 = \begin{bmatrix} 1 & 0 & 0 & 0 \\ 0 & 1 & 0 & 0 \\ 0 & 0 & 1 & 0 \\ 0 & 0 & 0 & 1 \end{bmatrix}, g_d = \begin{bmatrix} 1 & 0 & 0 & 20 \\ 0 & 1 & 0 & 0 \\ 0 & 0 & 1 & 0 \\ 0 & 0 & 0 & 1 \end{bmatrix}. \quad (24)$$

The plot of this maneuver can be seen in figure 1. It is a simple descent. To model disturbances, we added sinusoidal disturbances with 6-N amplitude and 0.13-Hz frequency, and constant disturbances with 1-N amplitude surge and sway motions as well as uniformly distributed random signals with 8-N amplitude to surge, sway, and heave motions, and constant disturbance with 5-N amplitude to heave motion. We then simulated this control scheme for $100s$.

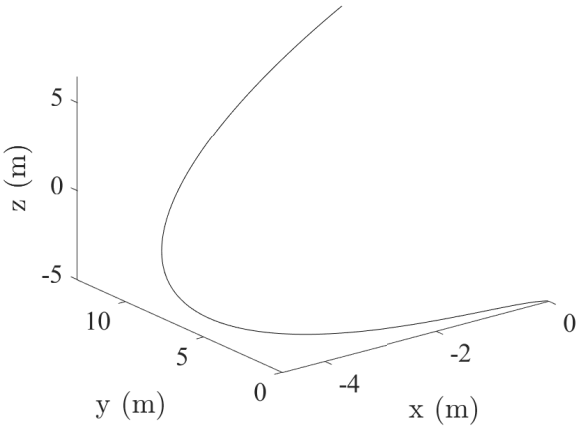

Fig. 1: Plot of the planned maneuver.

Applying the control (22) to the system (6), we obtain the position and orientation plotted in figure 2. The controller tracks the trajectory designed in figure 1 which moves the AUV from g_0 to g_d defined in (24) under the disturbances.

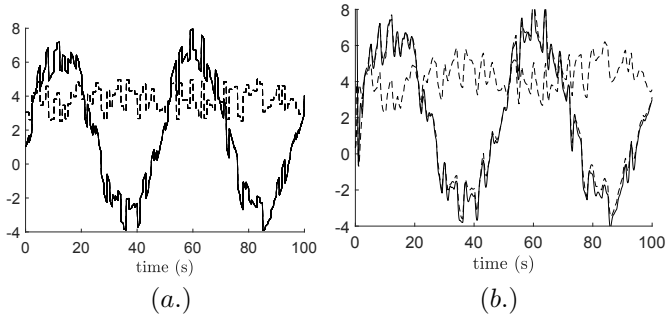

Fig. 2: Applied (a.) and (b.) measured disturbances

In figure 2 we plot the disturbances applied and the measurement of the disturbances. The observer tracks the disturbances accurately. In figure 3 we plot the error $\mathbf{V}_e$ under the outer-loop control and in the presence of disturbances. We can seen that the error remains small throughout the manouver.

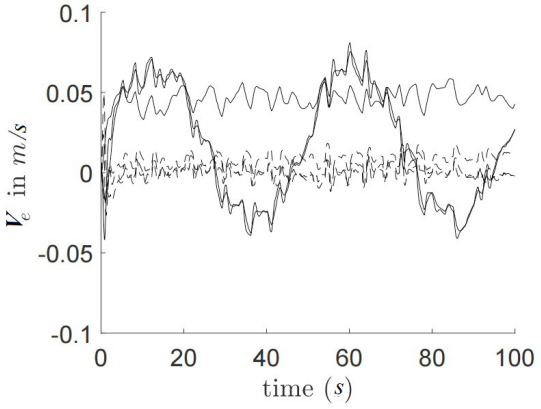

Fig. 3: Error $\mathbf{V}_e$ under tracking control.

4. CONCLUSIONS

In this study we designed and tracked an optimal trajectory for an underactuated AUV in the presence of time-varying disturbances and input saturation using a global representation of the position and orientation in $SE(3)$. Numerical shooting and inverse dynamics were applied to determine an inner-loop control to drive the AUV on the reference trajectory in perfect conditions; an additional outer-loop part was added to ensure convergence in the presence of bounded disturbances. The use of global coordinates also avoids singularities and so allows a more manouverable AUV to be modelled than local parametrizations (Sanyal et al (2011)). The simulations carried out demonstrate that even under strong perturbations (with magnitude of up to 8 N) the outer-loop control tracks the trajectory designed using the shooting method on $SE(3)$. It can also be seen that the trajectory that we designed is a simple spiral section. This approach could be applied to tracking for mechanical systems such as mobile robots by including the appropriate dynamics. A possible drawback of our method is that we assumed the position and attitude of the AUV are precisely known. However, in a real mission, there will be delays in the pose estimation. A specific area to be addressed in future work is the extension to include time delays and sensor uncertainties.

REFERENCES

I. R. Bertaska and K. D. von Ellenrieder. Experimental Evaluation of Supervisory Switching Control for Unmanned Surface Vehicles. IEEE Journal of Oceanic Engineering, 2018.

J. D. Biggs and W. Holderbaum. Optimal kinematic control of an autonomous underwater vehicle. IEEE transactions on automatic control 54.7, 1623-1626,2009

A. M. Bloch, et al. Geometric structure-preserving optimal control of a rigid body. Journal of Dynamical and Control Systems 15.3, 307-330, 2009

M. Candeloro, A. M. Lekkas, A. J. Sørensen and T. I. Fossen. Continuous Curvature Path Planning using Voronoi diagrams and Fermat's spirals. Proceedings of the 9th IFAC Conference on Control Applications in Marine Systems The International Federation of Automatic Control, Japan, 2013

W.H. Chen and L. Guo. Analysis of disturbance observer based control for nonlinear systems under disturbances with bounded variations. Proceedings of International Conference on Control, 1-5

W.H. Chen, J. Yang, L. Guo and Y. Sun. Disturbance-Observer-Based control and related methods - and overview. Automatica, 73, 207-214

K.D. Do Practical control of underactuated ships. Ocean Engineering, 37(13), 1111–1119, 2010

J, Du, X. Hu, M. Krstic and Y. Sun Robust dynamic positioning of ships with disturbances under input saturation. Automatica, 73, 207–214, 2016

T.I. Fossen and S. P. Berge. Nonlinear vectorial backstepping design for global exponential tracking of marine vessels in the presence of actuator dynamics. In Proc. 36th IEEE Conf. Decis. Control, 4237–4242, 1997

T. I. Fossen. Handbook of Marine Craft Hydrodynamics and Motion Control, First Edition. John Wiley & Sons Ltd. 2011

H. C. Henninger and J. D. Biggs. Optimal under-actuated kinematic motion planning on the ϵ-group. Automatica 90, 185-195,2018

H. C. Henninger and J. D. Biggs. A semi-analytic approach to spacecraft attitude guidance. 25th Mediterranean Conference on Control and Automation, Malta, July 3-6, 2017.

N.M. Horri and P. Palmer. Practical implementation of attitude-control algorithms for an underactuated satellite. Journal of Guidance, Control and Dynamics 35(1), 40–50,2012

V. Jurdjevic. Geometric Control Theory, UK: Cambridge University press, 1997

T. Lee, M. Leok and N. H. McClamroch Lie group variational integrators for the full body problem Computer Methods in applied mechanics and engineering, vol. 196, pp. 2907–2924, 2007

J. E. Marsden Lectures on mechanics, vol. 174 of London Mathematical Society Lecture Note Series Cambridge University Press, Cambridge, 1992.

N. Nordkvist and A. K. Sanyal A Lie Group Variational Integrator for Rigid Body Motion in SE(3) with Applications to Underwater Vehicle Dynamics. 49th IEEE Conference on Decision and Control, Atlanta, USA 2010

H. Nui and Z. Geng. Stabilization of an Underactuated AUV with Physical Damping on SE(3) via SIDA method. Proceedings of the 35th Chinese Control Conference,China,2016

Z. Pan and Z. Zhu. Miniature pipe robot. International Journal of Industrial Robotics, 30.6, 575–583, 2003.

T. J. Prestero. Verification of a six-degree of freedom simulation model for the REMUS autonomous underwater vehicle. PhD thesis, Massechusetts Institute of Technology, 2001

F. Rezazadegan, S. Shojaei and A. Chatraei. A novel approach to 6-DOF adaptive trajectory tracking control of an AUV in the presence of parameter uncertainties. Ocean Engineering, 107, 246–258,2015

A. Sanyal, N. Nordkvist and M. Chyba An Almost Global Tracking Control Scheme for Maneuverable Autonomous Vehicles and its Discretization IEEE transactions on automatic control, vol. 56, no. 2, February 2011

S. P. Viswanathan, A. K. Sanyal and M. Izadi Integrated Guidance and Feedback Control of Underactuated Vehicles in SE(3) American Institute of Aeronautics and Astronautics

S. Weißmann and U. Pinkall. Underwater rigid body dynamics. ACM Transactions on Graphics (TOG) 31.4,104,2012

J. Wu, J. Huang, Y. Wang and K. Xing Nonlinear disturbance observer-based dynamic surface control for trajectory tracking of pneumatic muscle system. IEEE Transactions on Control Systems Technology 22.2, 440-455, 2014

D. R. Yoerger and J-J E. Slotine. Robust Trajectory Control of Underwater Vehicles . IEEE Journal of Oceanic Engineering, Vol. OE-10- 4, 1985